Characterizing Soil Management Systems using Electromagnetic Induction.

Karl Vanderlinden[A], Gonzalo Martínez[A], Juan Vicente Giráldez[B] and José Luis Muriel[A]

[A]IFAPA, Centro Las Torres-Tomejil, Alcalá del Río (Seville), Spain, Email karl.vanderlinden@juntadeandalucia.es
[B]Dept. of Agronomy, University of Córdoba and IAS-CSIC, Córdoba, Spain

Abstract
Soil apparent electrical conductivity (EC_a) changes due to time-variant soil properties. A long-term soil management experiment was surveyed for EC_a on 13 occasions to capture changing soil conditions and to determine the sources of this variability. Especially subsoil EC_a patterns were found to exhibit temporal stability, while topsoil EC_a patterns were more variable, especially within the conventional tillage (CT) plots, in areas with shallow soils, and along the drainage network. The time-stable or mean EC_a pattern was associated with topography, soil depth and soil structure. The first three principal components explained 90% of the total variance and were related to the mean EC_a pattern, topography and soil management, respectively. Time-lapse images showed how tillage reduced EC_a in the CT plots, while it increased proportionally more then in the rest of the field when tillage was followed by low intensity rainfall, due to higher topsoil porosity and water content. High intensity rainfall caused a proportionally larger EC_a increment in the direct drill plots as a result of better infiltration conditions and runoff production in the CT plots. Electromagnetic induction sensors were found useful for mapping changing soil conditions as a result of soil management and external forcing.

Key Words
Electromagnetic induction, temporal stability, apparent electrical conductivity, time-lapse mapping, soil management, hydrological response.

Introduction
Mobile near-surface electromagnetic induction (EMI) sensors provide a non-invasive means for mapping soil apparent electrical conductivity (EC_a), which depends not only on time-invariant properties such as clay content, but also on time-variable soil properties such as water content and bulk density, among others (Friedman 2005). Tillage has a large effect on these time-variable properties, since it changes directly soil physical properties (Ahuja *et al*. 1998) and influences therefore the way a field responds to external forcing (*i.e*. rainfall and evaporation). As a consequence, EMI sensors can be used to monitor at the field scale changing soil conditions and to evaluate the impact of different soil management system. The objectives of this work were i) to check the existence of temporal stability of EC_a patterns in a long-term soil management experiment, ii) to identify independent sources of variability, and iii) to map changing soil conditions in response to soil management and external forcing.

Methods
Experimental field and mobile EMI sensor
The EC_a surveys were conducted at the *Tomejil* Farm long-term soil management experiment in SW Spain (Ordóñez *et al*. 2007), where the agronomical and environmental consequences of conventional tillage (CT), minimum tillage (MT) and direct drilling (DD) are being compared (Figure 1).

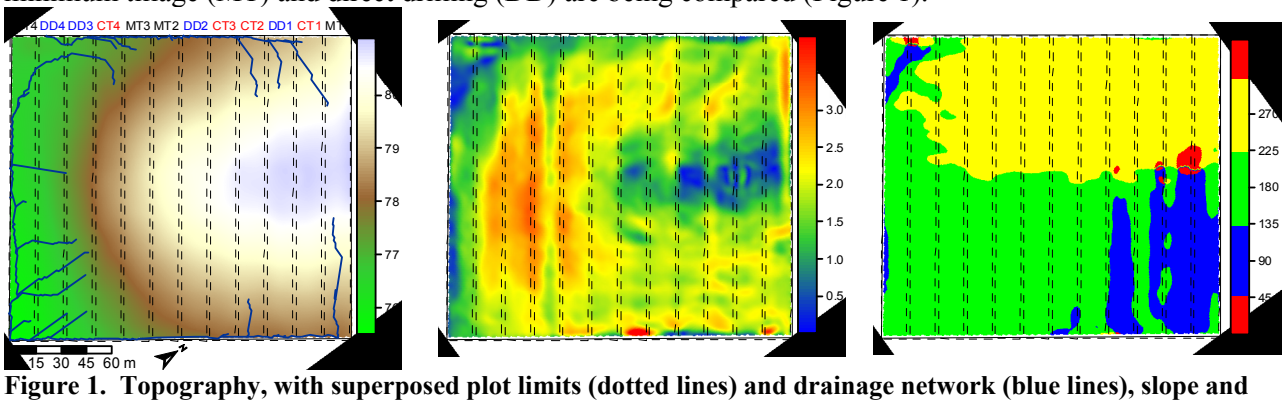

Figure 1. Topography, with superposed plot limits (dotted lines) and drainage network (blue lines), slope and aspect of the experimental field. MT: Minimum Tillage, CT: Conventional Tillage, DD: Direct Drill.

Four replicates of each treatment (15×180 m) were disposed in a completely random design within a 3.5 ha dry-land field under a wheat-sunflower-legume rotation. The soil is classified as a Chromic Haploxerert (Soil Survey Staff 1999) with topsoil clay and organic carbon contents of approximately 60% and 10 g/kg, respectively. The field was surveyed on 13 occasions between March 2006 and 2009, in-between harvest and sowing times, according to tillage and for different soil moisture conditions. Apparent electrical conductivity was measured using a EM38-DD EMI sensor (Geonics Inc, Ontario), which consists of a horizontally and vertically oriented dipole. The former provides topsoil (EC_{as}) and the latter subsoil EC_a measurements (EC_{ad}). The sensor was hosted in a protected PVC sled and pulled by an ATV, equipped with a RTK-DGPS receiver, a guidance bar for parallel swathing at 3 m and a field computer to log the EC_a data, coordinates and elevation with a frequency of 1Hz.

ECa data analysis

Point EC_a measurements were interpolated using Ordinary Kriging with local variogram calculation (Minasny *et al*. 2002). In order to integrate and facilitate the comparison of EC_{as} and EC_{ad} maps for different measurement campaigns, interpolated data were transformed to relative differences, δ_{ij}, as described by Vachaud *et al*. (1985):

$$\delta_{ij} = \frac{EC_{aij} - \langle EC_a \rangle_j}{\langle EC_a \rangle_j}, \quad (1)$$

where EC_{aij} is the EC_a at point (pixel) *i* and survey time *j*, and $\langle EC_a \rangle_j$ is the spatial average of the field on survey time *j*. For each location *i* the mean relative difference, $\overline{\delta_i}$, of the 13 measurement campaigns and its standard deviation, $\sigma_{\delta i}$, were calculated in order to evaluate the temporal persistence or rank stability of the EC_a patterns. Principal component analysis (PCA) was used to extract independent patterns from the 13 $\overline{\delta}$ maps for EC_{as} and EC_{ad}, representing a large part of the total variability of both data sets. PCA scores were mapped for the three first PC´s and used to identify the main sources of variation by associating them with physical attributes of the field. Patterns of EC_a changes were obtained by differencing δ maps of consecutive surveys, $\Delta_{\delta i} = \delta_{ij} - \delta_{ik}$, where *k* and *j* are two consecutive measurement campaigns (Robinson *et al*. 2009).

Results

ECa data

The spatial mean EC_{as} and EC_{ad} for the 13 surveys ranged from 27 to 84 and from 80 to 137 mS/m, with mean values of 59 and 104 mS/m, respectively. The extreme values for EC_{as} and EC_{ad} were observed on different days, indicating different topsoil and subsoil dynamics. In general, higher EC_a values were observed during wet periods (e.g. Nadler 2005), while the lowest values were found during dry periods, after summer and harvest. Changes of spatial mean EC_{as}, were higher since the main causes of temporal variability such as drying-wetting (and shrinkage-swelling), tillage and root development occur mainly in the topsoil. In general, probability density functions of both EC_{as} and EC_{ad} were close to normal or slightly positively skewed, as a consequence of high EC_a values in the lowest part of the field, where water and sediments accumulated as a result of surface and subsurface flow.

Temporal persistence of ECa patterns.

The mean relative difference maps for EC_{as} and EC_{ad} showed similar patterns [Figure 2 (a-b)], indicating that both dipole orientations can be used to map the mean, time-stable, EC_a pattern of the field. The observed pattern was associated with topography (drainage network), depth to the underlying marl, and aggregate shape. EC_a values in the eastern corner of the field were about 40% higher than the spatial mean since this is a low area. On the other hand, an area in the eastern corner of the field could be identified where EC_a values were 20% smaller than the spatial mean. Here, the depth to the underlying marl was found to be larger and aggregates were found to be prismatic in contrast to the platy or blocky aggregate shape found in the rest of the field, leading to a better drainage capacity and dryer soil conditions. The rest of the field showed EC_a values within ±10% of the spatial mean, with higher values in plot MT4 due to its position within the drainage network, and in a part of plot MT3, as a consequence of a smaller soil depth. The associated σ_δ maps [Figure 2 (c-d)] show a better temporal stability for the EC_{ad} data, since most of the factors affecting time-variable soil properties are more active in the topsoil layer. As expected temporal stability was generally worse in the CT plots, in areas with a shallow soil, and along the drainage ways.

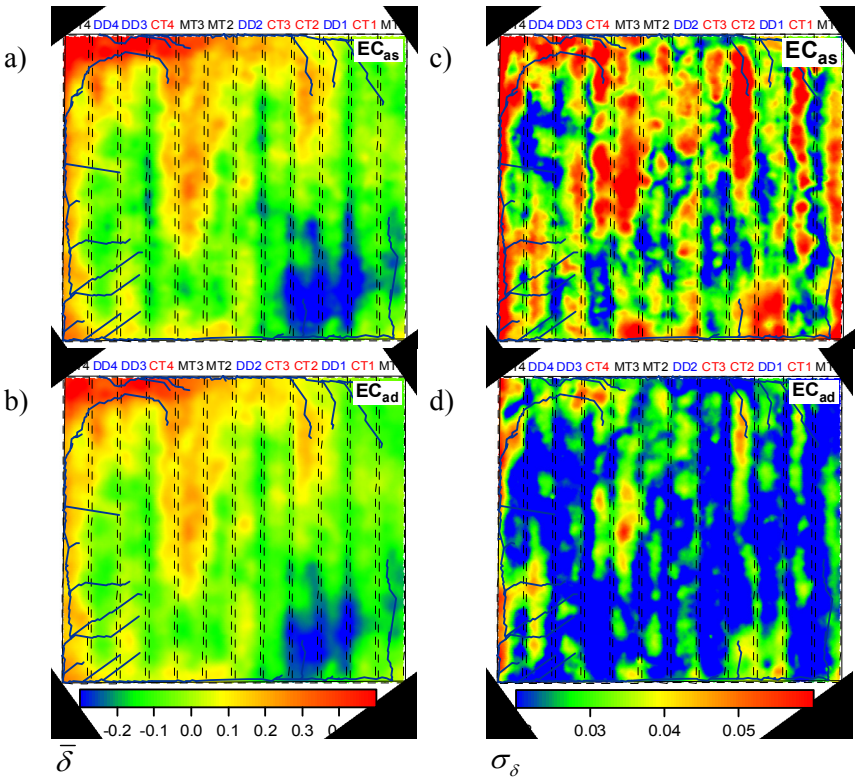

Figure 2. Mean relative difference, $\bar{\delta}$, and corresponding standard deviation, σ_δ, calculated from the 13 EC_a surveys, in horizontal (EC_{as}) and vertical dipole mode (EC_{ad}).

Principal component analysis

The first three PC´s represented about 90% of the total variance. For EC_{as} they accounted for 65, 14 and 11%, and for EC_{ad}, 74, 13 and 6% of the total variance, respectively. Figure 3 shows that the pattern of PC I corresponded with the mean, time stable, EC_a pattern, as shown in the $\bar{\delta}$ maps of figure 2. The pattern of the second component could be roughly related with topographical attributes such as slope and aspect, while PC III showed a pattern related with soil management.

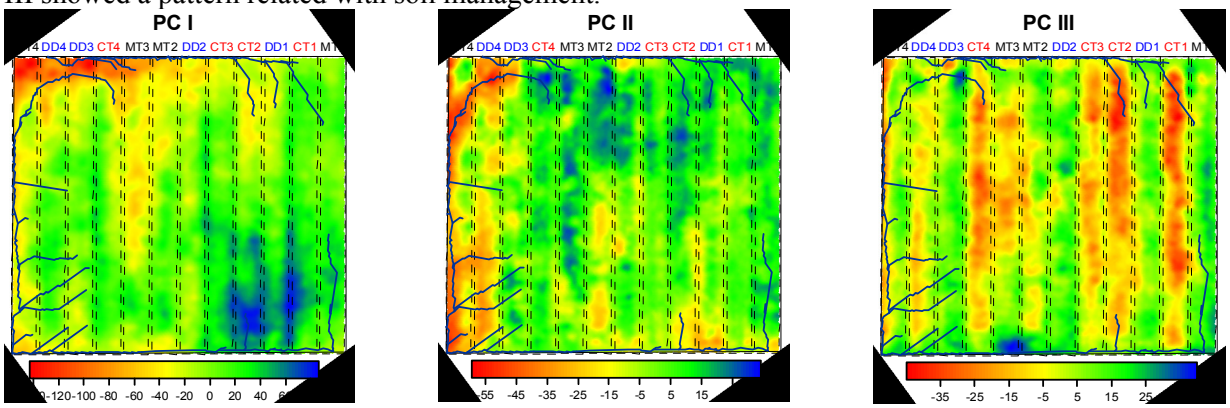

Figure 3. Maps of the scores of the first three principal components, representing 65, 14 and 11 % of the total variability, respectively, as calculated from the 13 EC_{as} surveys.

Patterns of changing ECa

Figure 4 (a-b) shows the EC_{as} and EC_{ad} Δ_δ maps calculated from surveys on 08.09.18 and 08.11.10, where mouldboard ploughing in CT and disc harrowing in MT on 08.10.06 caused a proportionally larger decrease of EC_a in the CT plots due to the plow-generated porosity. The largest differences could be observed in the EC_{as} Δ_δ map since topsoil EC_a especially decreased after tillage. However, tillage followed by low intensity rainfall caused proportionally larger Δ_δ values in the CT plots, especially for EC_{as}, as a result of the higher porosity and the presence of a plough pan [Figure 4 (c-d)]. The Δ_δ maps in figure 4 (e-d) clearly show how the different soil management systems responded to a single intense rainfall event (115 mm). Proportionally larger increments can be observed in the DD plots as a result of higher soil water content increments. The

existence of better infiltration conditions in the DD plots favored the recharge of the soil profile and avoided runoff production, in contrast to the MT and CT plots where significant runoff and sediment yield was observed.

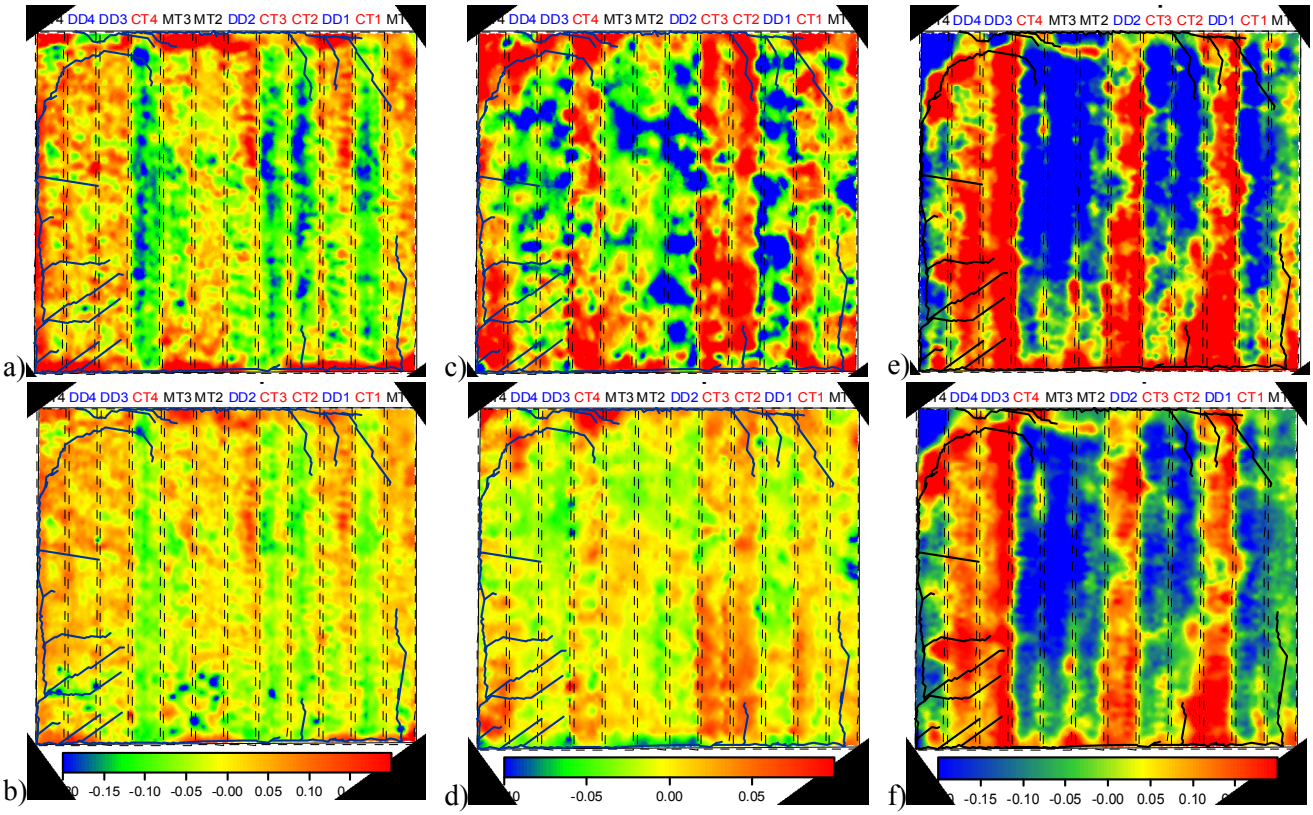

Figure 4. Differenced δ EC_a, Δ_δ, maps calculated from surveys on 08.09.18 and 08.11.10 (a-b), 06.03.10 and 06.03.29 (c-d), and 07.11.07 and 07.11.29 (e-f), showing the effect of ploughing, the combined effect of ploughing and low intensity rainfall and the effect of high intensity rainfall, respectively. Maps in the upper row (a, c, e) are for EC_{as}.

Conclusion

The time-stable, mean pattern, obtained from 13 EC_a surveys of an experimental field could be related with topographical characteristics, soil depth and soil structure, while the mean pattern, the interaction of topography with soil water content, and soil management were identified as independent sources of variability, explaining 90% of the total variability of the spatio-temporal datasets. The electromagnetic induction sensing system used here was found very adequate for mapping changes in EC_a-related time-variable soil properties such as soil water content or porosity and can therefore be used to compare the spatially distributed performance of different soil management systems at the field scale.

References

Ahuja LR, Fiedler F, Dunn GH, Benjamin JG, Garrison A (1998) Changes in soil water retention curves due to tillage and natural reconsolidation. *Soil. Sci. Soc. Am. J.* **62,** 1228-1233.

Friedman SP (2005) Soil properties influencing apparent electrical conductivity: a review. *Comput. Electron. Agric*. **46,** 45–70.

Minasny B, McBratney AB, Whelan BM (2002) *Vesper* (Variogram Estimation and Spatial Prediction plus Error) version 1.6. Australian Centre for Precision Agriculture. http://www.usyd.edu.au/su/agric/acpa.

Nadler A (2005) Methodologies and the practical aspects of the bulk soil EC (σ_a)–soil solution EC (σ_w) relations. *Adv. Agron*. **88,** 275–312.

Ordóñez R, González P, Giráldez JV. Perea F (2007) Soil properties and crop yields after 21 years of direct drilling trials in southern Spain. *Soil Tillage Res*. **94,** 47–54.

Robinson DA, Lebron I, Kocar, B, Phan K, Sampson M, Crook N, Fendorf S (2009) Time-lapse geophysical imaging of soil moisture dynamics in tropical deltaic soils: An aid to interpreting hydrological and geochemical processes. *Water Resour. Res*. **45,** W00D32, doi:10.1029/2008WR006984.

Soil Survey Staff (1999) *Soil Taxonomy*. 2nd edition. USDA Ag. Hbk. 437, Washinton.

Vachaud G, Desilans AP, Balabanis P, Vauclin M (1985) Temporal stability of spatially measured soil-water probability density-function. *Soil Sci. Soc. Am. J*. **49,** 822–828.